Analysis of Nonaxisymmetric Modes in Accretion Disks at Marginal Stability with Nonlinear Diffusion and Dissipation *

T. Islam and B. Coppi

Massachusetts Institute of Technology

A class of unstable modes with azimuthjal wavenumber, in accretion disks with an equilibrium magnetic field $\mathbf{B} \simeq B_\phi(R,z)\mathbf{e}_\phi + B_z(R,z)\mathbf{e}_z$, that can transport angular momentum have the following properties: they are radially localized over distances much smaller than R, the radius of the disk; they require the effects of finite pressure for their excitation; they possess two sets of singularities in the MHD approximation; and they require a localized diffusion or dissipation operator to resolve the inner singularity [1,2]. The spectrum of modes about marginal stability was analyzed numerically for linear operators and reported in Ref. [3], where the existence of separate classes of solutions with different numbers of nodes in the radial direction was demonstrated.

Nonlinear diffusion and dissipation operators have been proposed on the basis of the fact that within the inner singularities, pressures and densities tend to infinity and therefore nonlinear effects become important [4]. The MHD equation describing the radially ballooning nonaxisymmetric modes [1, 2, 5] is modified into one that smoothly connects the solution within the transition regions to the MHD solution outside the transition regions [3]. The physical basis of nonlinear operators described in a previous report [4] is discussed. For the nonlinear operators, the marginal stability condition is analyzed by taking the ratio δ of the width of the transition layers to the radial extent of the mode to be much less than 1, and the growth rate to be of order δ relative to the orbital frequency. A spectrum of modes, with different numbers of radial nodes, is mapped for each of the nonlinear operators.

[1] B. Coppi and P. S. Coppi, *Ann. Phys.* **291**, 134 (2001).

[2] B. Coppi and P. S. Coppi, *Phys. Rev. Lett.* **87**, 051101 (2001).

[3] R. Bhatt, B. Coppi, I. Dimov, and J. Gagnon, *Bull. Am. Phys. Soc.* **45**, 38 (2000).

[4] B. Coppi and P. S. Coppi, M. I.T. (R. L. E.) Report PTP-01/04 (2001).

[5] B. Coppi and P. S. Coppi, *Phys. Lett. A* **239**, 261 (1998); B. Coppi and P. S. Coppi, M. I. T. (R. L. E.) Report PTP-97/08 (1998).

*Supported in part by the U. S. Department of Energy

Magnetorotational Instability

The magnetorotational instability (MRI)[1, 2] was reintroduced in the study of magnetized accretion disks[3] as a fast, powerful mode to transport angular momentum in accretion disks that are *stable* to the rotational instability.

- transports particles and angular momentum in MHD plasma.
- maximum growth rate $\gamma \sim \Omega$.
- wavenumber of fastest modes $k \sim v_A/\Omega$.
- diffusion coefficient $D \equiv k^{-2}\gamma \sim \alpha_{SS} c_s H$[4], where $\alpha_{SS} = v_A^2/c_s^2 \equiv$ Shakura-Sunyaev α parameter.

And has been applied to thick disks, which are capable of supporting a large range of MRI modes, due to their large width $\sim$ radius.

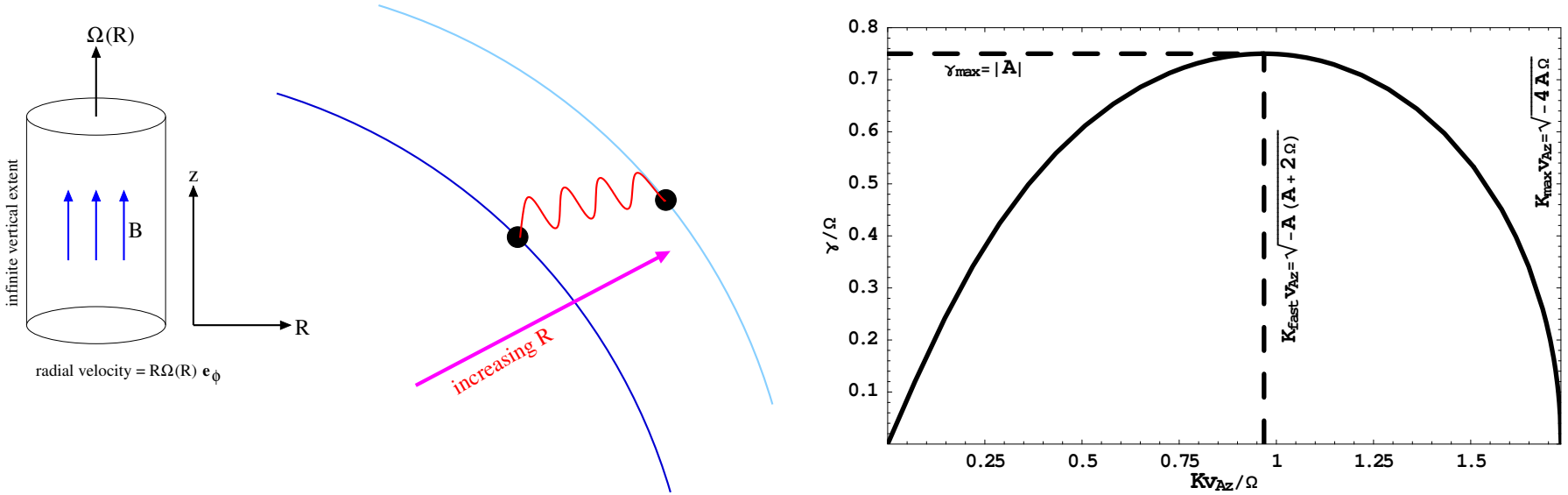

Figure 1: On left is a cartoon of the MRI in which the disk is infinitely thick vertically, and the mode is of the form $\hat{\xi} = \tilde{\xi}\exp(ik_z z + \gamma t)$, with equilibrium magnetic field $\mathbf{B} = B_z \mathbf{e}_z$. The magnetic tension, with resulting frequency $k_z^2 v_A^2$, where $v_A^2 = B_z^2/4\pi\rho$ is the Alfvén frequency and ρ is the fluid density, between two fluid elements at adjacent radii acts as a "spring" connecting them and driving the MRI at sufficiently small wavenumbers k_z.
On right is the growth rate of MRI for a Keplerian disk $\Omega(R) \propto R^{-3/2}$. Here $A = -\frac{3}{2}\Omega = Rd\Omega/dR$; maximum growth rate is of the order Ω, the orbital rotation frequency, and maximum wavenumber $k_z v_A \sim \Omega$.

Nomenclature

$v_A^2 = \dfrac{B^2}{4\pi\rho}$, Alfvén speed	$c_s^2 \equiv$ sound speed.	$\lambda_0 = \dfrac{\gamma_0}{\omega_{A_s}}$
$A_s = \dfrac{v_A^2}{c_s^2}$	$\omega_A = k_\parallel v_A$, shear Alfvén wave	$\omega_{A_s} = k_\parallel \sqrt{\dfrac{v_A^2 c_s^2}{v_A^2 + c_s^2}}$, magnetosonic wave
$\alpha_k = \dfrac{2}{3}\left\lvert\dfrac{d\ln\Omega}{d\ln R}\right\rvert$, rotational shear	$\alpha_z = \dfrac{3B_\phi}{2B_z}\alpha_k$,	$\delta_0 = \dfrac{\omega_{A_s}}{\lvert n^0\Omega'\rvert} = -\dfrac{\omega_{A_s}}{\Omega k_z \alpha_z}$,
$r = \dfrac{R - R_0}{\delta_0}$,	$K_s = \dfrac{\omega_{A_s}}{b_\phi \Omega}$	$D_T = D_\mu + \dfrac{D_m c_s^2}{c_s^2 + v_A^2} + \dfrac{D_p v_A^2}{c_s^2 + v_A^2}$ total diffusion coeff.

- D_μ refers to kinetic viscous diffusion coefficient.
- $D_m = \eta c^2/4\pi$ refers to magnetic diffusion coefficient (where η is the cgs plasma resistivity).
- D_p refers to the thermal diffusion coefficient.

Justification and Form for 3D (Nonaxisymmetric) Modes

- For thin disks, the appropriate instabilities are ballooning modes: [5, 6, 7, 8, 9]
  $\hat{v}_R \simeq \tilde{v}_R(z) \exp\left(\gamma_0 t + i k_R \left(R - R_0\right)\right)$.
  - they are characterized by $\Delta_R \ll \Delta_z \ll H$, disk height.
  - This requires that $v_A^2 \ll c_s^2$, limiting applicability.
  - Properly localized mode (i.e. mode decreases as quickly in z or quicker than density) with *discrete* eigenmodes (discrete values of k_R, γ_0); therefore, it is difficult to construct radially localized packets.

- Axisymmetry imposes a strict condition between k_R and variation in z – since the disk is *thin*, the width of modes vertically $\Delta_z < H$, and k_R must be very large.

- Introducing nonaxisymmetric modes – azimuthal dependence – allows for an extra degree of freedom. One can choose that combination of total wavenumber in ϕ and z such that magnetic field lines are minimally bent, i.e. $\mathbf{k}\cdot\mathbf{B} \ll kB$, where $k = \sqrt{k_z^2 + n^{0^2}/R^2}$ and $B = \sqrt{B_z^2 + B_\phi^2}$. Form of the 3D nonaxisymmetric modes are then given by:

$$\hat{A}(R, z, \phi, t) = \tilde{A}(R) \exp\left(i k_z z + i n^0 \phi - i\omega t\right)$$

With equilibrium magnetic field $\mathbf{B} \simeq B_\phi \mathbf{e}_\phi + B_z \mathbf{e}_z$.

Model of the Thin, Ionized Non-Self Gravitating Accretion Disk

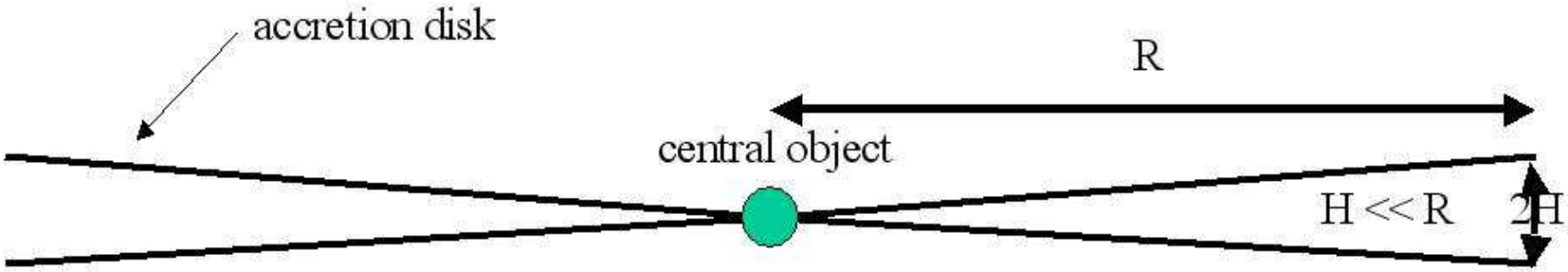

- gravity dominated by the central object, So $\Omega \propto R^{-3/2}$, where
  Ω is orbital frequency
  R is disk radius

- Radial magnetic fields $B_R << B_\phi, B_z$.

- Thin accretion disk ($H << R$), so $v_{th} << v_\phi$, where
  H is disk height
  v_{th} is thermal velocity
  $V_\phi = R\,\Omega$ is orbital velocity

- Largely ionized disk and long mean free paths – justifying collisionless MHD equations throughout the disk.

Mode Properties[6, 10]

- Eigenmodes with eigenvalues K_s are found for which $\mathrm{Re}\,\tilde{\xi}$ is even, $\mathrm{Im}\,\tilde{\xi}$ is odd.
- These modes are excited for relatively large magnetic energy densities, $v_A^2 \sim c_s^2$.
- Mode is localized over distances $\delta_0 = \omega_{A_s}/(\Omega k_z \alpha_z) \sim k_\parallel H/k_z \ll R$ about the corotation point, where $n^0\Omega(R) = \mathrm{Re}(\omega)$.

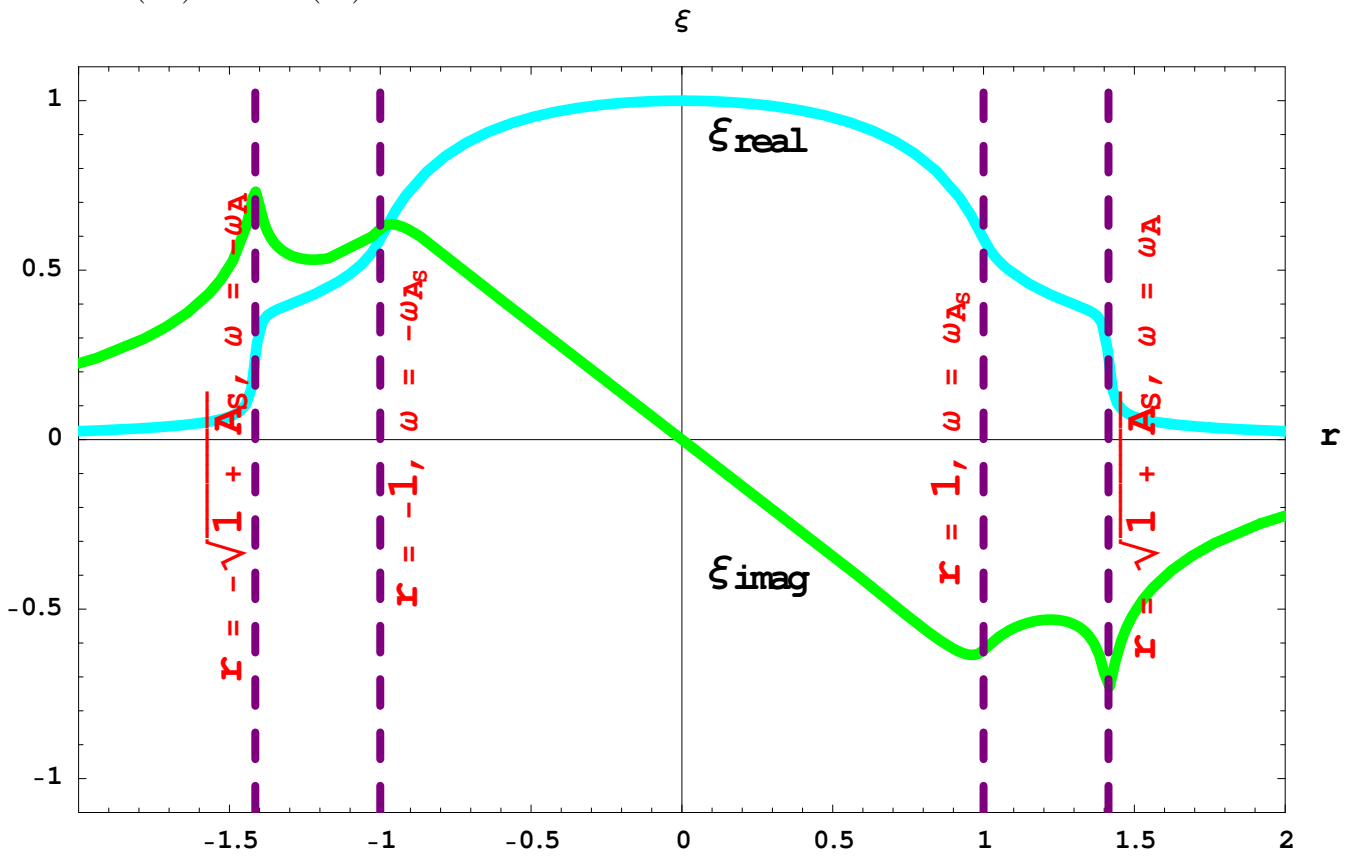

In the MHD approximation to the mode, singularities appear at radii $R - R_0 = \pm\delta_0$ (doppler shift $\bar{\omega} = \pm\omega_{A_s}$) and at $R - R_0 = \pm\delta_0\sqrt{1 + A_s}$ (doppler shift $\omega = \pm\omega_A$).

Master Equation

- One can form a single-variable dispersion equation that reproduces the behavior in r about the singularities at $r^2 = 1$ and $r^2 = 1 + A_s$, preserving the parity of the solution in $\tilde{\xi}$:

$$-\alpha_z^2 \frac{d}{dr}\left(\left[(r-r_b)^2 - 2i\Gamma_0\delta_1\,(r-r_b)\right]\frac{d\tilde{\xi}}{dr}\right) \simeq$$

$$\left[K_s^2\left[1 + A_s - r^2 + 2i\Gamma_0\delta_1 r\right] + \frac{3\alpha_k + (4-3\alpha_k)\left(r^2 - 2i\Gamma_0\delta_1 r\right)}{(r-1)^2 - 2i\Gamma_0\delta_1\,(r-1) + \dfrac{2\delta_1}{Z\left\{(r-1)/\delta_1\right\}}}\right]\tilde{\xi}$$

  Where the effects of a finite smoothing operator are not necessary in resolving the second singularity (see, e.g., [7, 6, 11] for other examples). Here $\lambda_0 = \Gamma_0\delta_1$ is the normalized modal growth rate, and the physical size of the transition region $\Delta_1 = \delta_1\delta_0$.

- The smoothing operator that describes the inner transition region:

$$(\hat{x} - i\Gamma_0)\,Z(\hat{x}) + i\mathcal{O}_{\text{even}}Z(\hat{x}) = 1$$

  Where $\mathcal{O}_{\text{even}}$ is some operator even in $\hat{x}$, such that the partity of the solution is preserved.

Linear and Nonlinear Transition Models

- The characteristic function that is used to determine range of normalized growth rates $\Gamma_0 = \lambda_0/\delta_1$ [6, 10]:

$$\mathcal{I}(\Gamma_0) = \int_{-\infty}^{\infty} \mathrm{Im}\, Z(x;\Gamma_0)\, dx \propto \frac{1}{\mathrm{Im}\,\xi(1)} \left(\left.\frac{d\mathrm{Im}\,\tilde{\xi}}{dr}\right|_{r=1^+} - \left.\frac{d\mathrm{Im}\,\tilde{\xi}}{dr}\right|_{r=1^-} \right)$$

  One uses a transition operator $\mathcal{O}_{\mathrm{even}}$ such that $\mathcal{I}(\Gamma_0) \neq \pi$, allowing for instability range $0 < \Gamma_0 < \Gamma_0^{\max}$.

  Unlike the simple diffusion operator as seen in magnetic reconnection, this operator must be "localized" (have varying dissipation rate or diffusion coefficient) about the inner singularity [6, 7, 8]. ***A diffusion operator of the form*** d^2/dx^2 ***results in*** $\mathcal{I}(\Gamma_0) = \pi$***, hence a constant jump in the*** $\tilde{\xi}$ ***derivative as a function of*** Γ_0.

- For those modes whose transition is described by *linear* diffusion or dissipation operators, with collisional diffusion coefficients:
  - Small growth rates given by following:

$$\gamma_0 \sim \omega_{A_s}^{2/3} \left(D_T \delta_0^{-2}\right)^{1/3} = \left(D_T k_z^2 \Omega^2 \alpha_z^2/2\right)^{1/3} \ll \omega_{A_s}$$

  - The width of the transition layers:

$$\Delta_1 = \left(D_T/\left(2k_z\Omega\alpha_z\right)\right)^{1/3} \ll \delta_0$$

- For nonlinear transition regions (which may arise due to the effects of large pressures, densities at the inner $(R-R_0)^2 = \delta_0^2$ transition region), one may get the following [8].
  - The transition layer thickness $\delta_1 = \left|\tilde{\xi}(r=1)/L_N\right|^{1/2}$.
  - Growth rate $\gamma_0 \sim \Omega B_\phi/B \left|\tilde{\xi}(r=1)/L_N\right|^{1/2}$.

  In the limit that the fluid displacement $\left|\tilde{\xi}(r=1)\right| \gg L_N\delta_1^2$, where L_N is the *threshold fluid displacement* for the appearance of nonlinear effects.

Examples Solutions of 3D Modal Equation

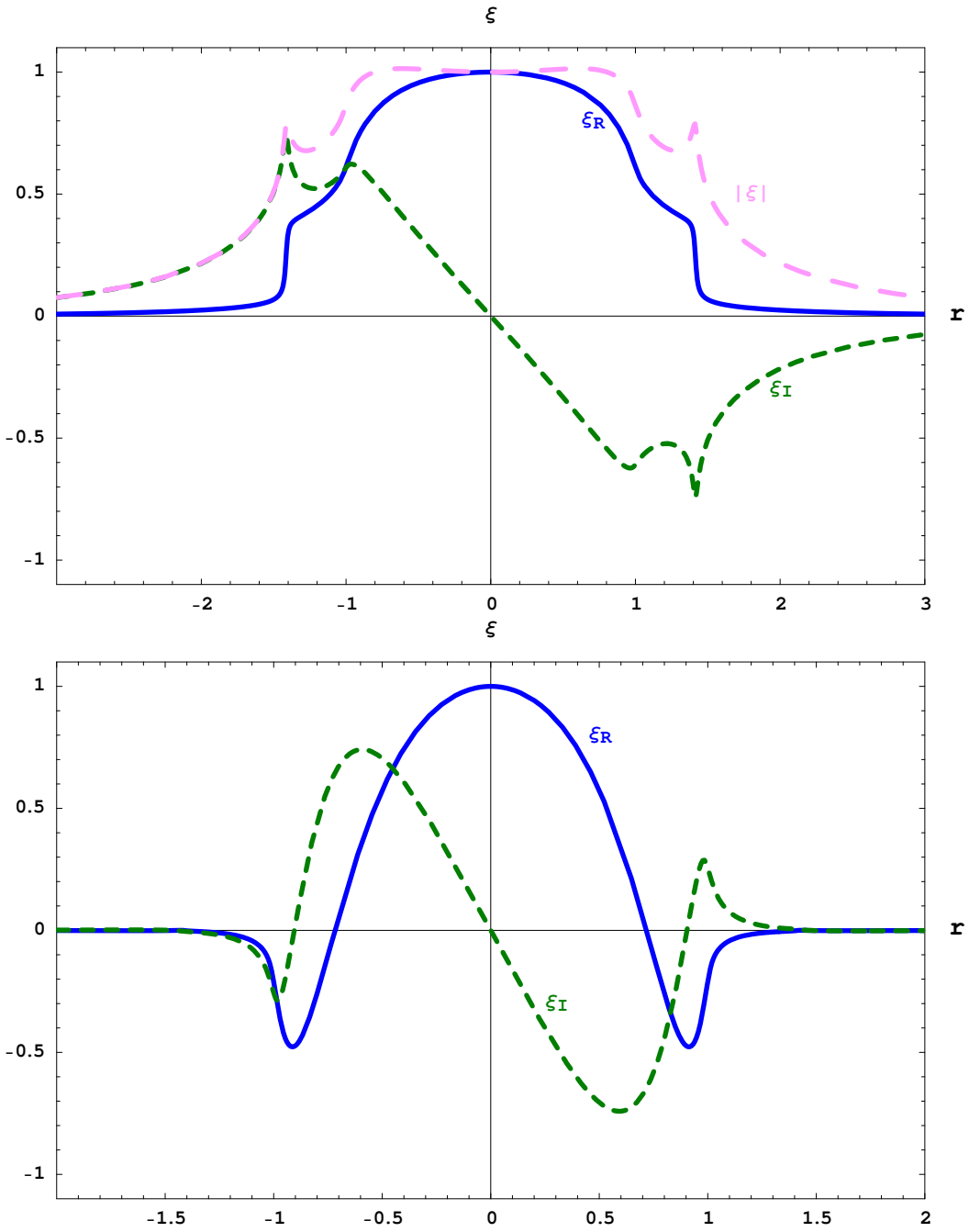

On *top* is a **zero-node** eigensolution to the 3D modal equation with a representative linear smoothing operator, and on the *bottom* is a **one-node** eigensolution with the same smoothing operator. Note that $\tilde{\xi}_I \equiv \mathrm{Im}\,\tilde{\xi}$ is an odd function while $\tilde{\xi}_R \equiv \mathrm{Re}\,\tilde{\xi}$ is an even function in r. The number of nodes is defined as the number of times $\tilde{\xi}_I$ crosses the r axis for $r > 0$. The one node solution resides at smaller α_z than the zero-node solution, with all other parameters in the 3D modal equation being kept equal.

The Linear Operator (As a Basis of Comparison) *

The smoothing operator that describes a "linear" dissipation is a simplification of the simplest smoothing operator that was described in [5, 7]. In this case, the smoothing operator is given by:

$$(\hat{x} - i\Gamma_0)\, Z(\hat{x}) - \frac{i\nu_{0L}}{\hat{x}^2} Z(\hat{x}) = 1$$

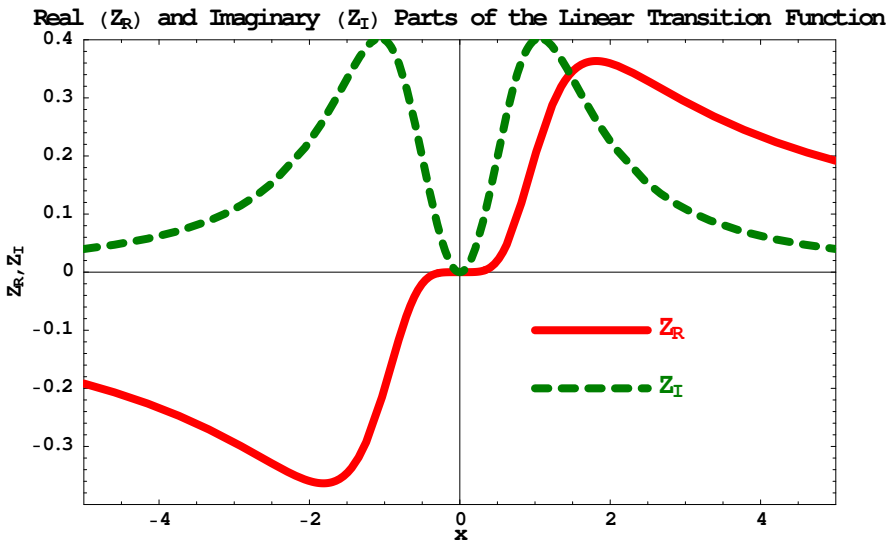

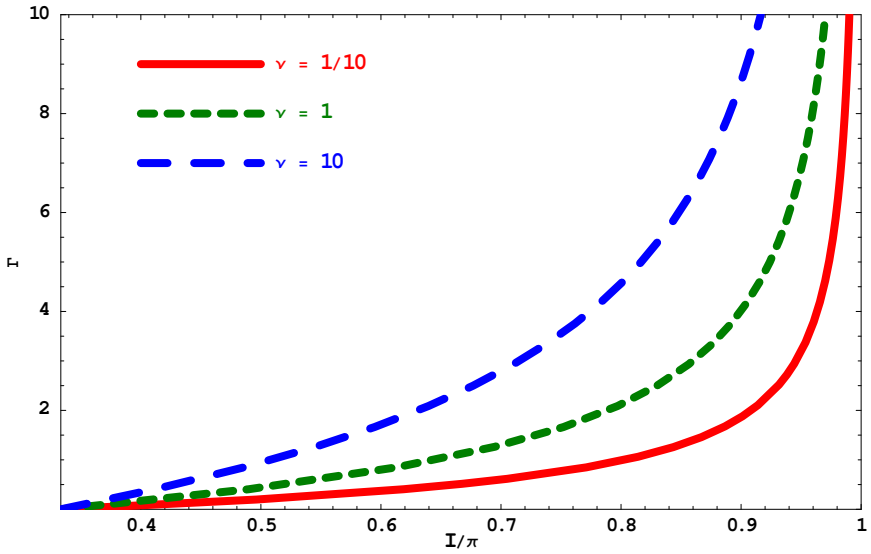

Plot of the transition function Z_I ($\mathrm{Im}\, Z(x)$) and Z_R ($\mathrm{Re}\, Z(x)$) for $\Gamma_0 = 1$ (on left) and the relation $\mathcal{I} = \int_{-\infty}^{\infty} Z_I(x)\, dx$ as a function of ν_{0L} and Γ_0, for $0 \leq \Gamma_0 \leq \infty$. Here $\lim_{\Gamma_0} \mathcal{I}(\Gamma_0) \to 1/3$.

*The eigenmodal analysis using this transition model is denoted as **linear #1**

Diffusive Nonlinear Model[†]

A simple nonlinear diffusion (diffusion because of second derivatives d^2/dx^2 in the transition equation) model that has a wide range of $\mathcal{I}(\Gamma_0)$ as Γ_0 is varied is given by:

$$xZ_R + \Gamma Z_I - \left(\int_{-\infty}^{\infty} Z_I(x)\, dx \right) \frac{d^2 Z_I}{dx^2} = 1 \qquad\qquad xZ_I - \Gamma Z_R = 0$$

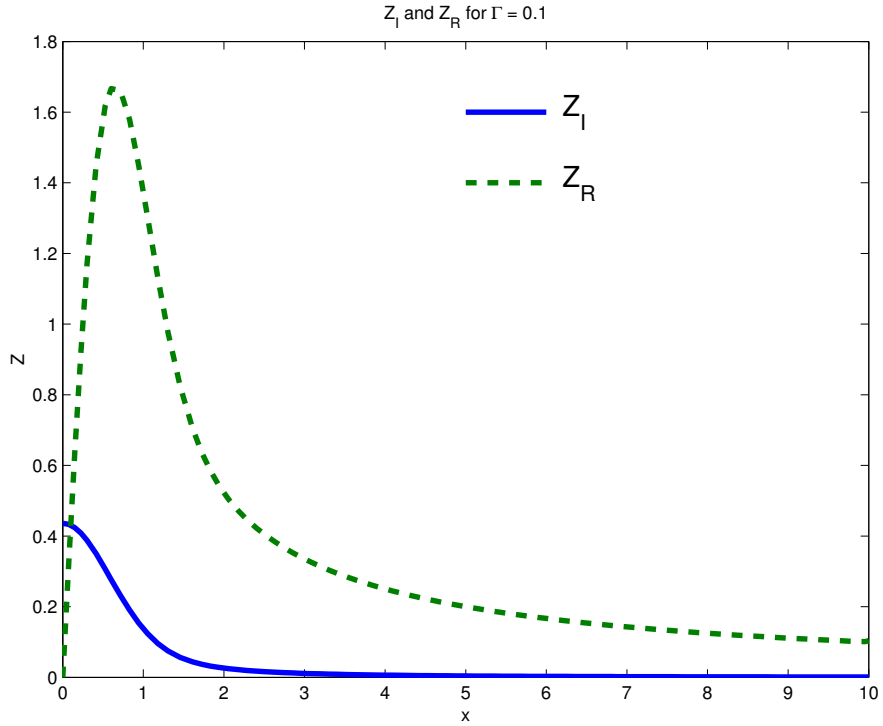

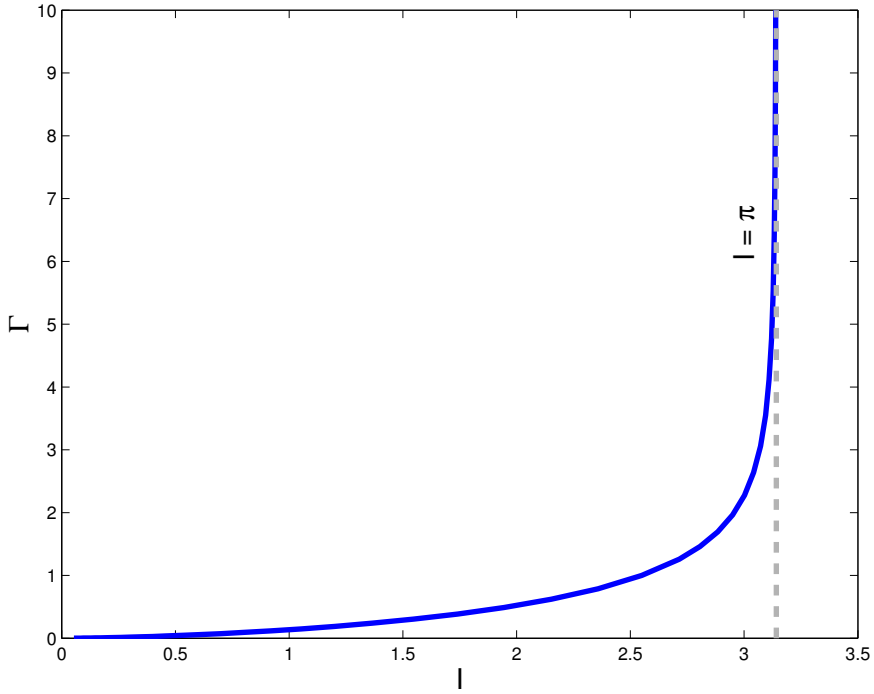

Plot of the imaginary and real parts of $Z(x)$, Z_I and Z_R, for $\Gamma_0 = 0.1$ (on left) and the relation $\mathcal{I}(\Gamma_0)$ for $10^{-6} \leq \Gamma_0 \leq 10$.

[†]The eigenmode analysis denoted by this simple nonlinear diffusion model is denoted as **nonlinear #1**

Simple Dissipative Nonlinear Model[‡]

A dissipative nonlinear model, first introduced and justified in [8], is described by the following transition equation:

$$(x - i\Gamma_0)\, Z(x) - |Z|^2 = 1$$

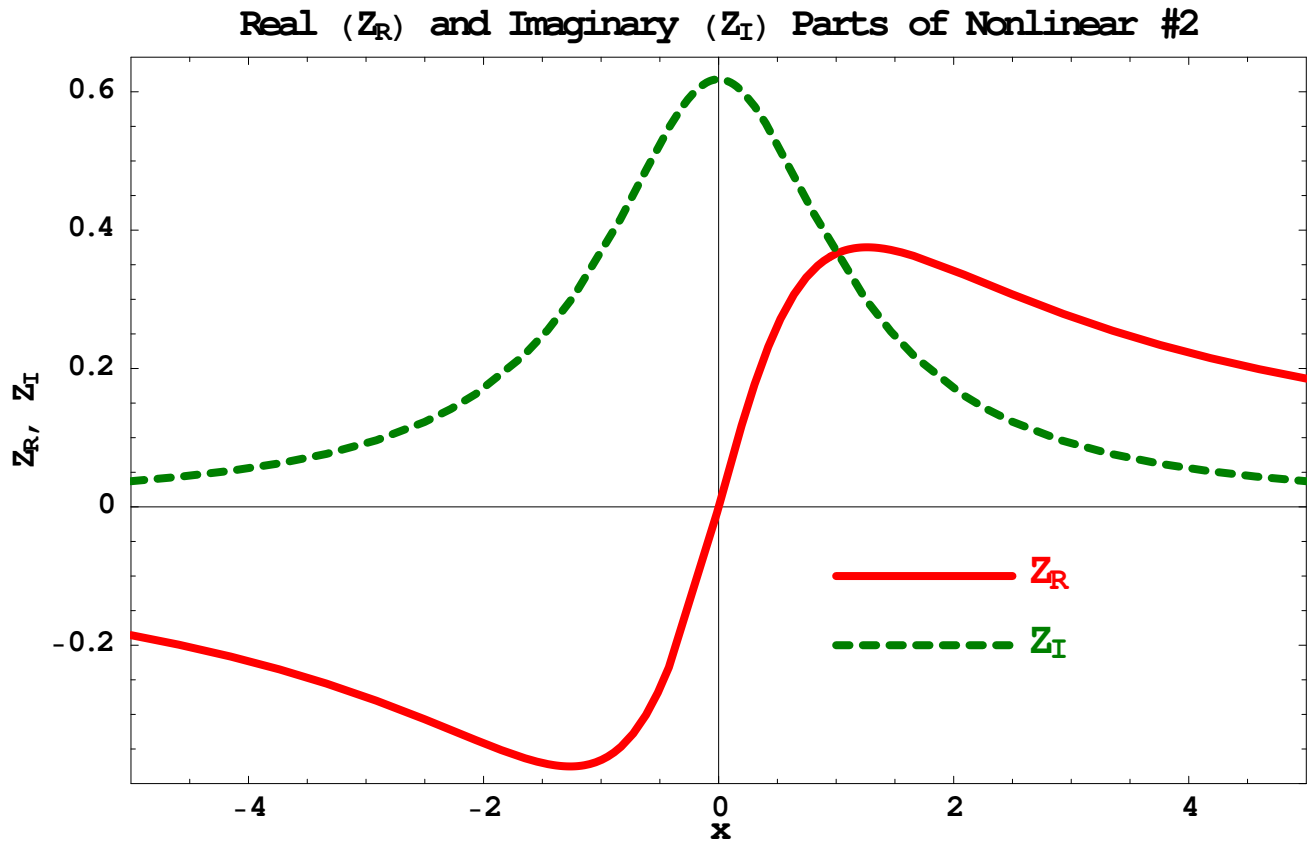

Plot of the imaginary and real parts of $Z(x)$, Z_I and Z_R, for $\Gamma_0 = 1$ in the simple nonlinear dissipation function. From an analytic study, one finds that $\mathcal{I}(\Gamma_0) \approx 2.2\Gamma_0$.

[‡]The eigenmode analysis denoted by this simple nonlinear diffusion model is denoted as **nonlinear #2**

Trends For Linear #1 Transition Model

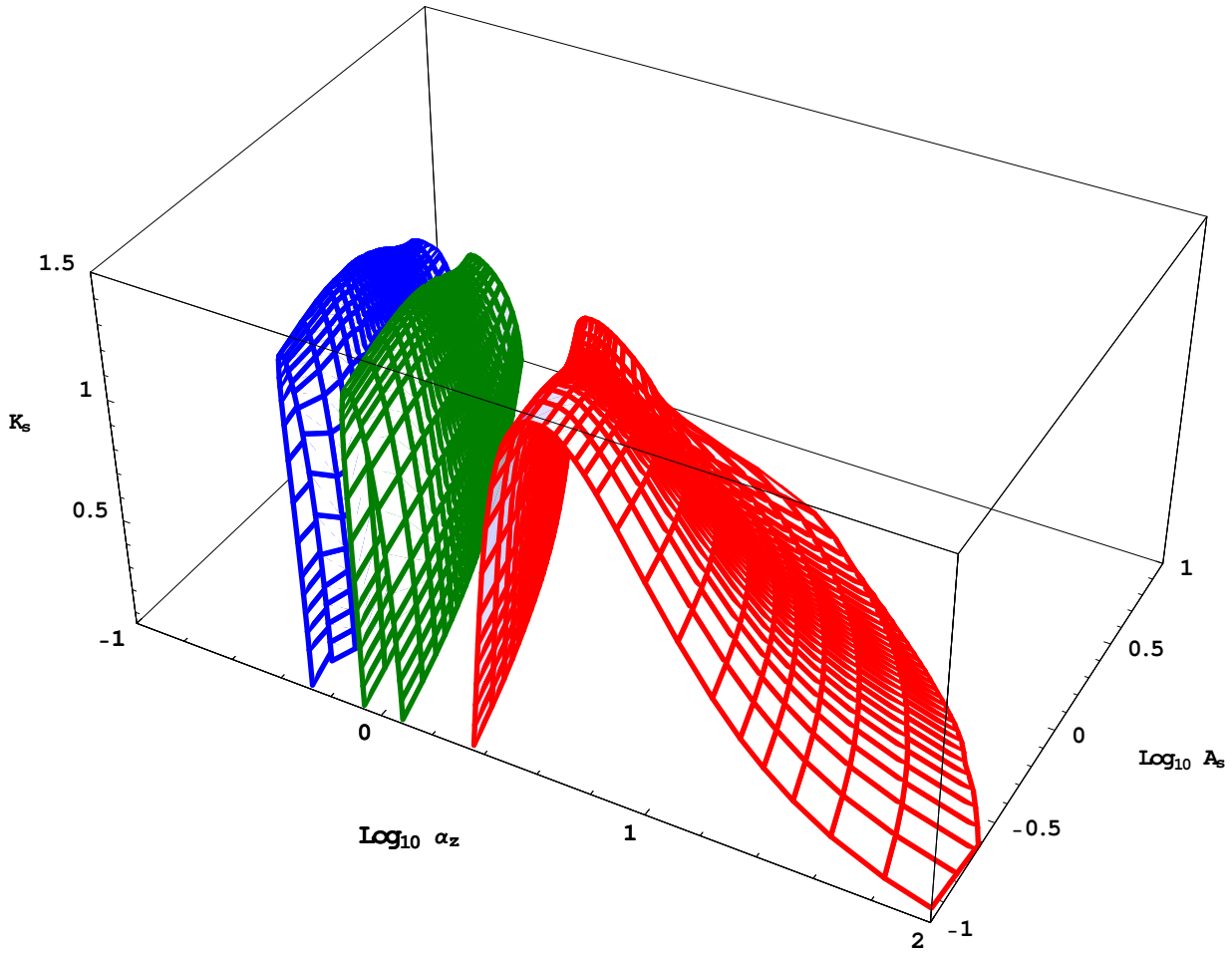

In **red** is shown the zero-radial node solutions, in **green** the one radial node, and in **blue** the two-radial node solutions, as A_s is varied from $1/10 \leq A_s \leq 10$, for the linear transition model *linear #1*. Here $\lambda_0 = \Gamma_0 \delta_1 = 10^{-3}$ (hence $\Gamma_0 = 1$), and the trend to lower values of K_s is seen as A_s is varied, keeping all other paramaters constant.

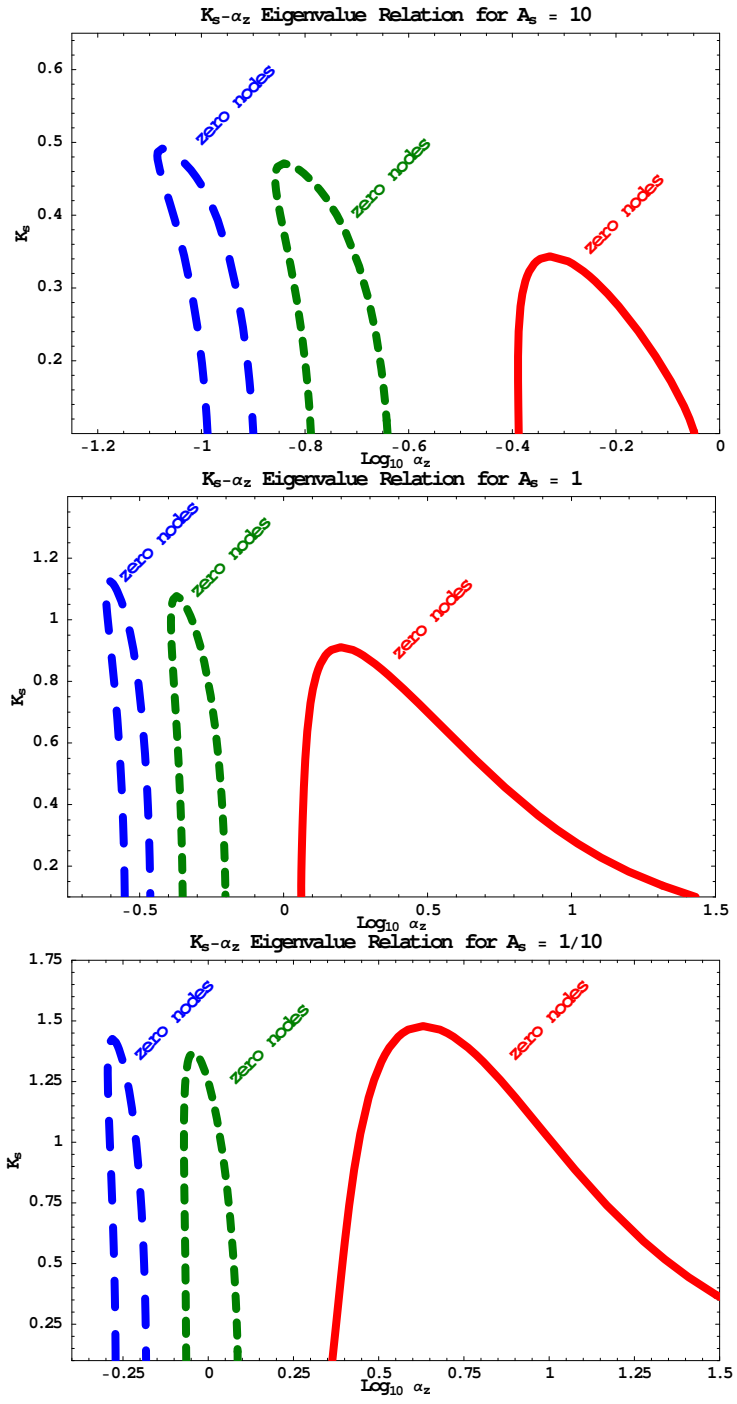

A more explicit map of the eigenvalue $K_s - \alpha_z$ relation for the linear smoothing operator *linear #1*, varying A_s while keeping $\lambda_0 = \Gamma_0 \delta_1 = 10^{-3}$ and $\delta_1 = 10^{-3}$ constant. As first shown in [5, 7], as A_s increases (magnetic energy dominating over thermal energy), the modes have decreased K_s and they exist at lower α_z – hence in a more toroidal field. Equivalently, for all three nodal eigenvalues, as A_s, the K_s decreases – hence the parallel wavenumber $k_\parallel$ becomes smaller.

Furthermore, especially for large A_s it appears that there exist "double" solutions – two values of K_s for a given growth rate Γ_0 and equilibrium field, represented by α_z – a result that could not be easily observed in previous work on marginally stable 3D modes [5].

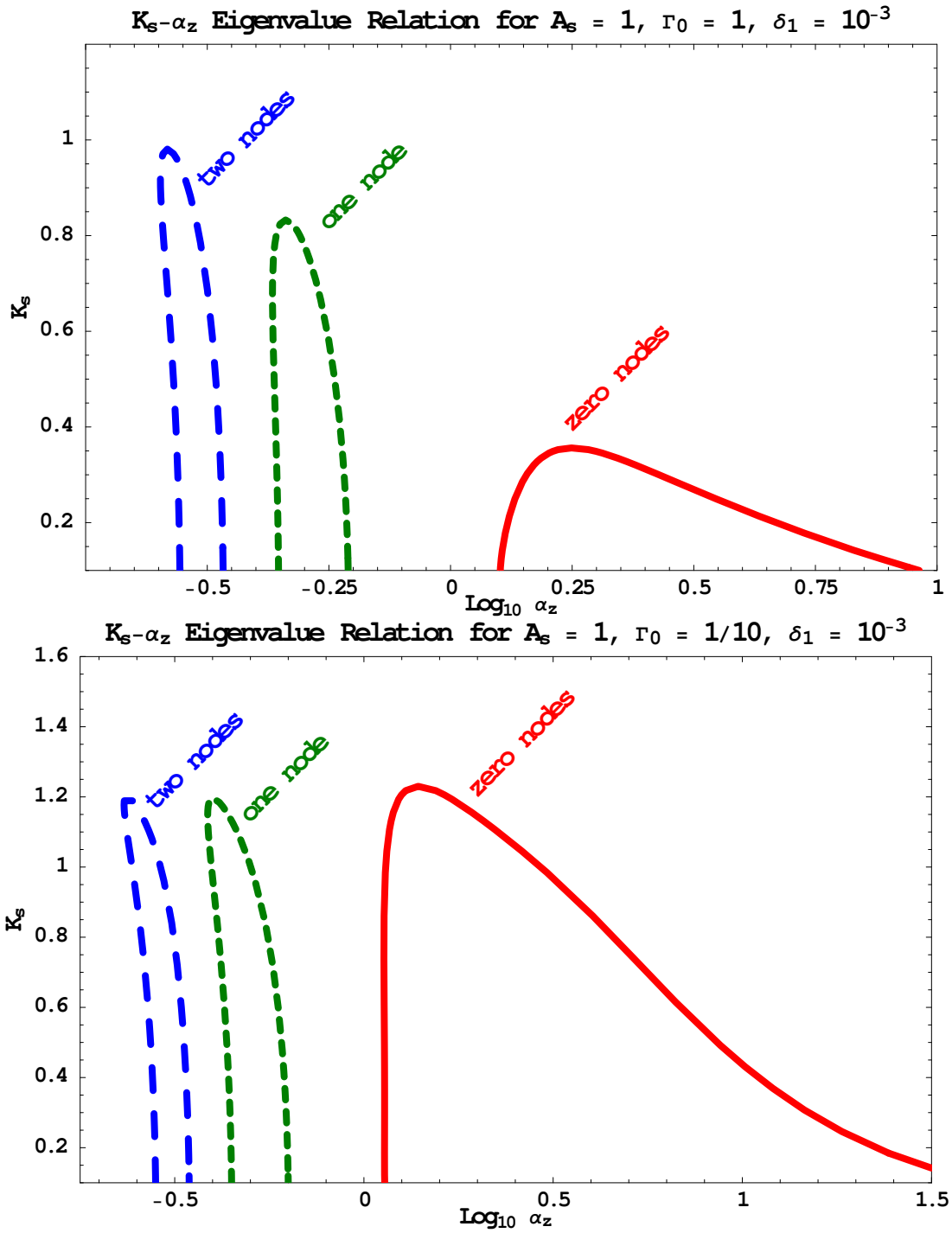

The $K_s - \alpha_z$ relation for the linear smoothing operator *linear #1*, for the case where $\lambda_0 = 10\delta_1 = 10^{-2}$ (on top, high growth rate) and for the case where $\lambda_0 = 0.1\delta_1 = 10^{-4}$ (on bottom, low growth rate), keeping $A_s = 1$. As confirmed in [5, 7], the effects of increasing the growth rate decreases K_s, as well as shifting the various nodal eigensolutions to higher α_z (more toroidal magnetic fields).

Trend For Nonlinear #1 Transition Model

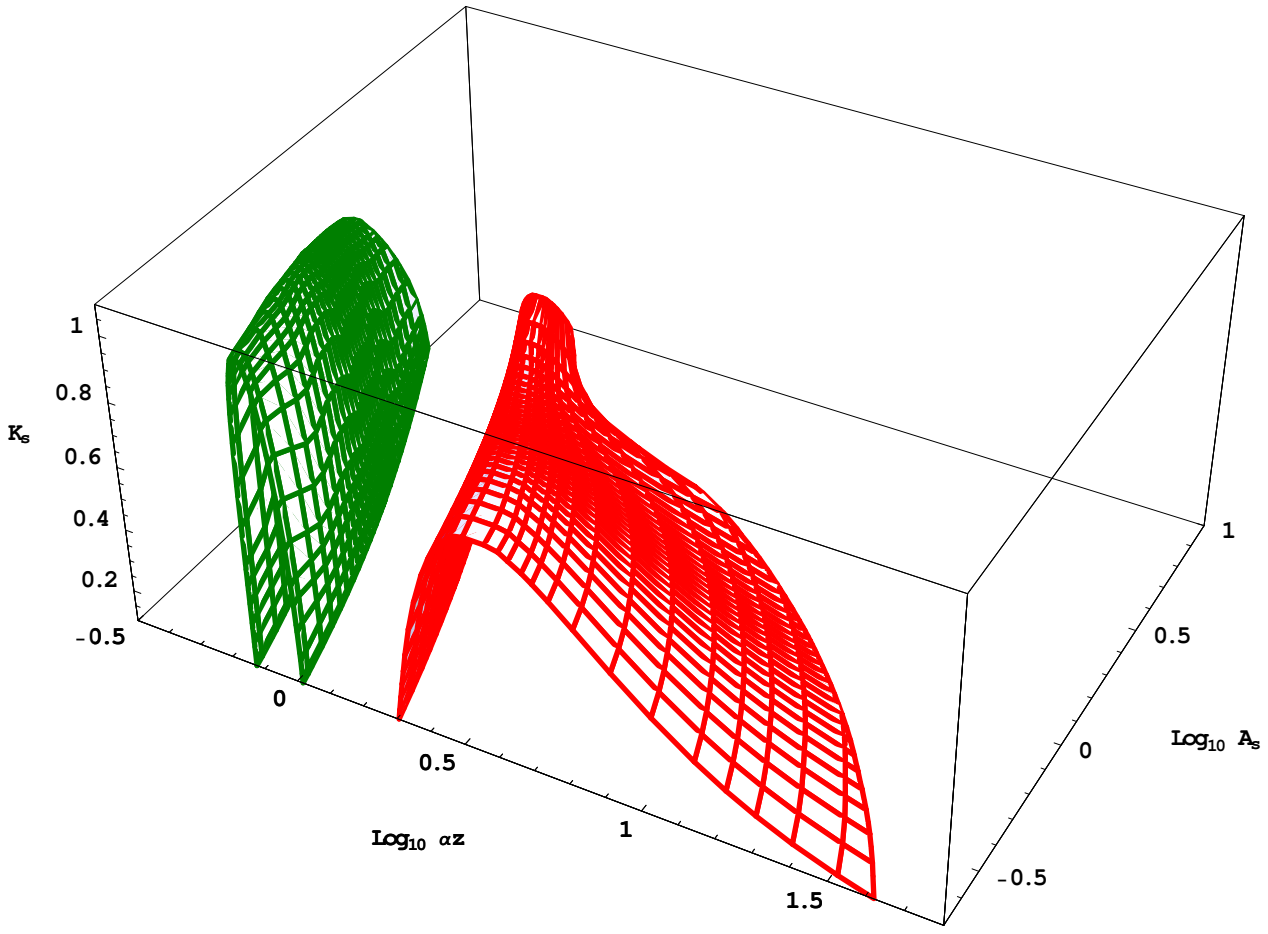

In **red** is shown the zero-radial node solutions and in **green** the one radial node, as A_s is varied from $1/10 \leq A_s \leq 10$, for the nonlinear diffusive transition model *nonlin #1*. Here $\lambda_0 = \Gamma_0 \delta_1 = 10^{-3}$ (hence $\Gamma_0 = 1$), and the trend to lower values of K_s is seen as A_s is varied, keeping all other paramaters constant.

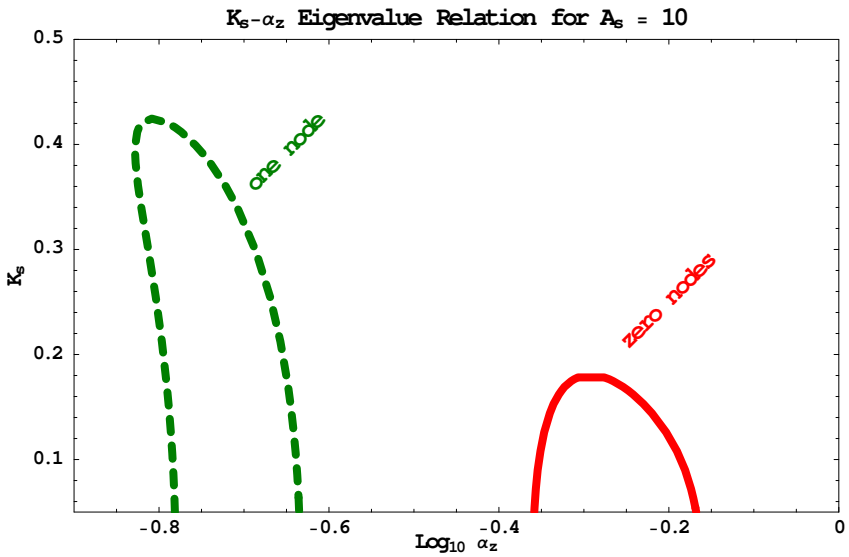

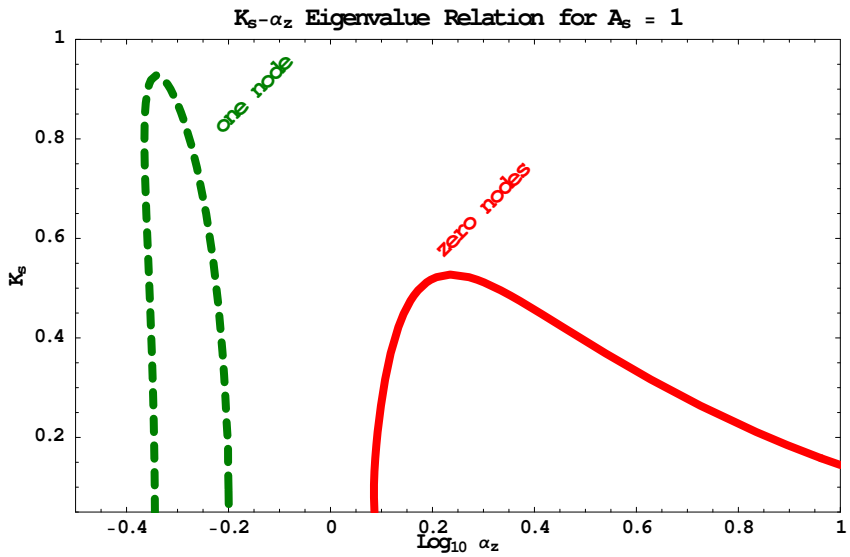

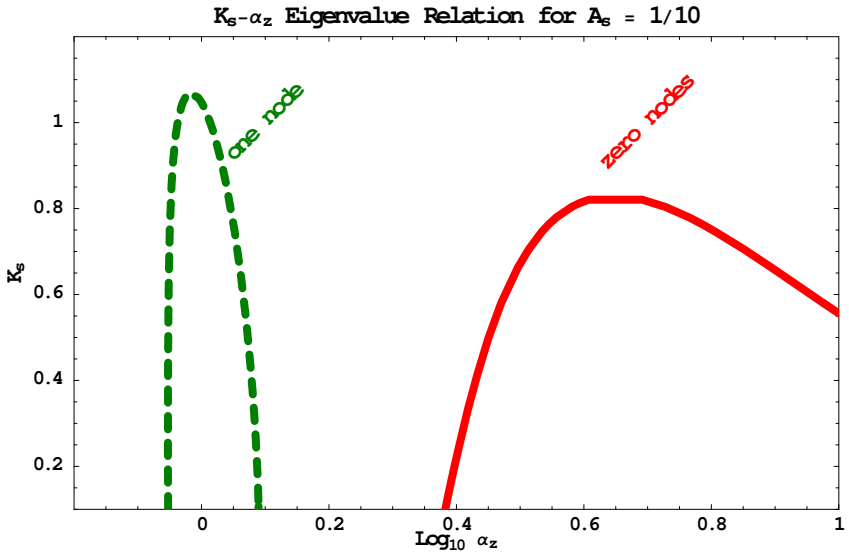

A more explicit map of the eigenvalue $K_s - \alpha_z$ relation for the diffusive nonlinear smoothing operator *nonlin #1*, varying A_s while keeping $\lambda_0 = \Gamma_0 \delta_1 = 10^{-3}$ and $\delta_1 = 10^{-3}$ constant. The behavior in α_z and K_s of the nodal solutions is the same as in *linear #1*.

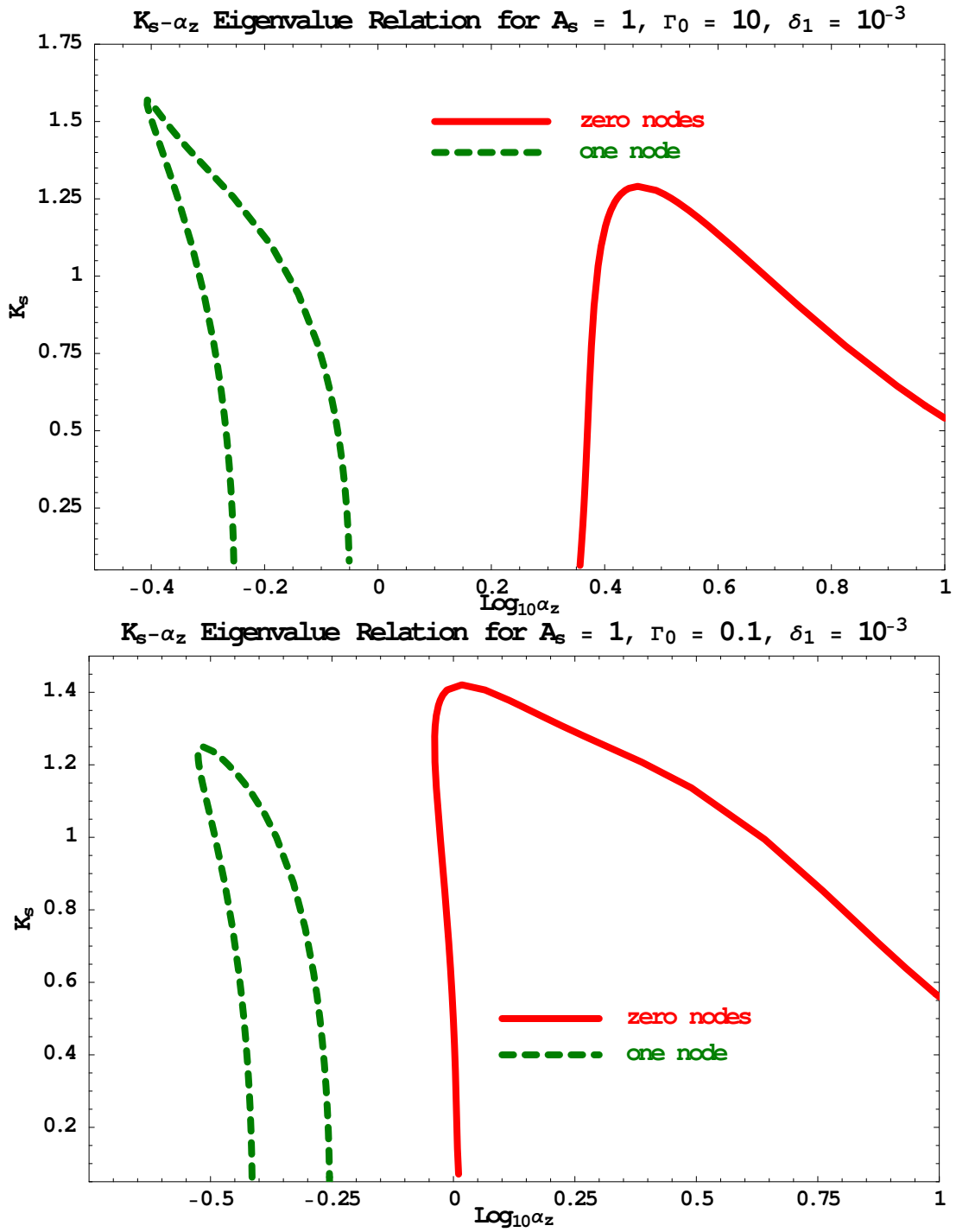

The $K_s - \alpha_z$ relation for the nonlinear diffusive smoothing operator *nonlinear #1*, for the case where $\lambda_0 = 10\delta_1 = 10^{-2}$ (on top, high growth rate) and for the case where $\lambda_0 = 0.1\delta_1 = 10^{-4}$ (on bottom, low growth rate), keeping $A_s = 1$. The trend in K_s and α_z as the the growth rate Γ_0 is varied is the same as in *linear #1*, although the change in K_s for each node is not as severe .

Trends For Nonlinear #2 Transition Model

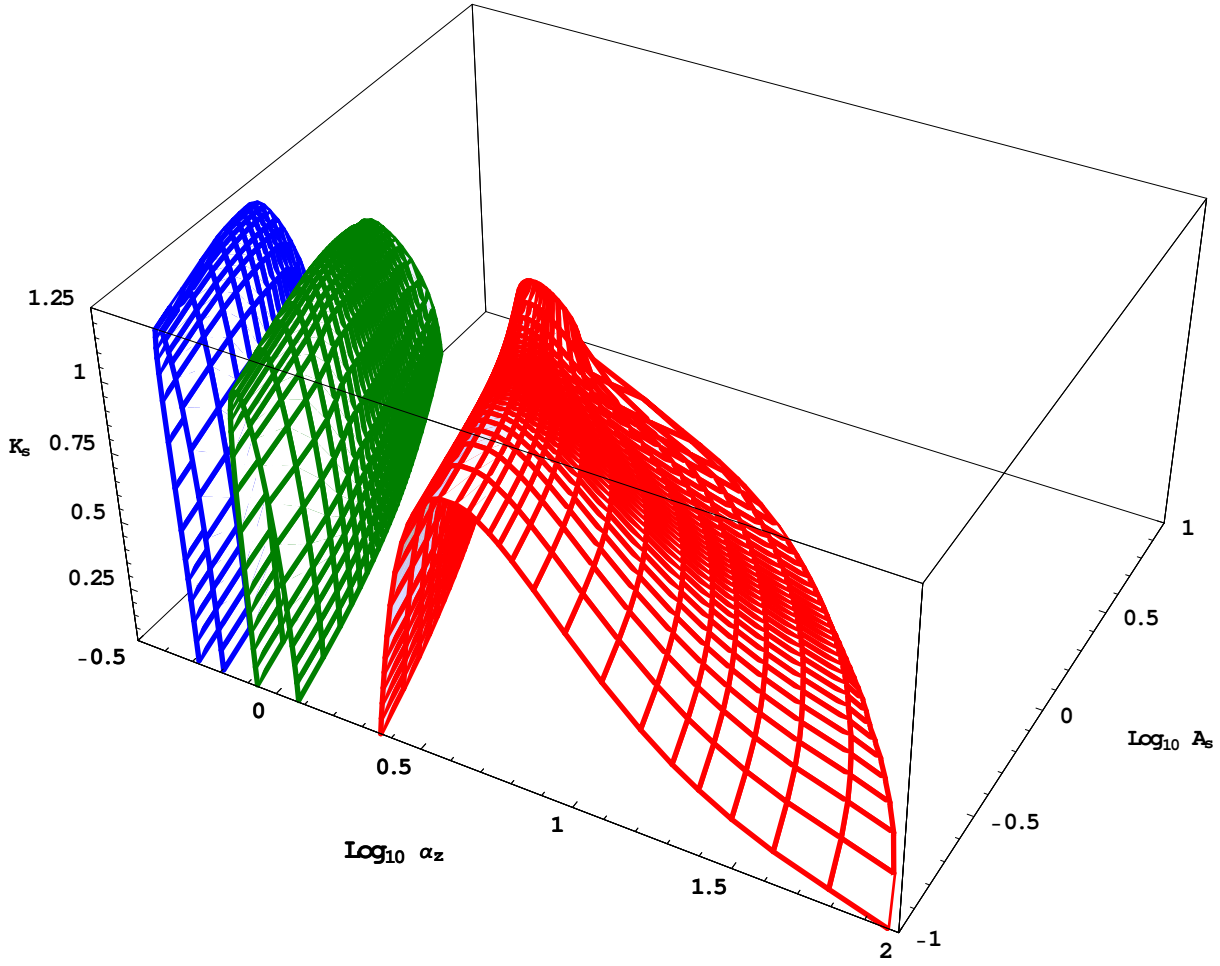

In **red** is shown the zero-radial node solutions, in **green** the one radial node, and in **blue** the two-radial node solutions, as A_s is varied from $1/10 \leq A_s \leq 10$, for the dissipative nonlinear transition model *nonlin #2*. Here $\lambda_0 = \Gamma_0 \delta_1 = 10^{-3}$ (hence $\Gamma_0 = 1$), and the trend to lower values of K_s is seen as A_s is varied, keeping all other paramaters constant.

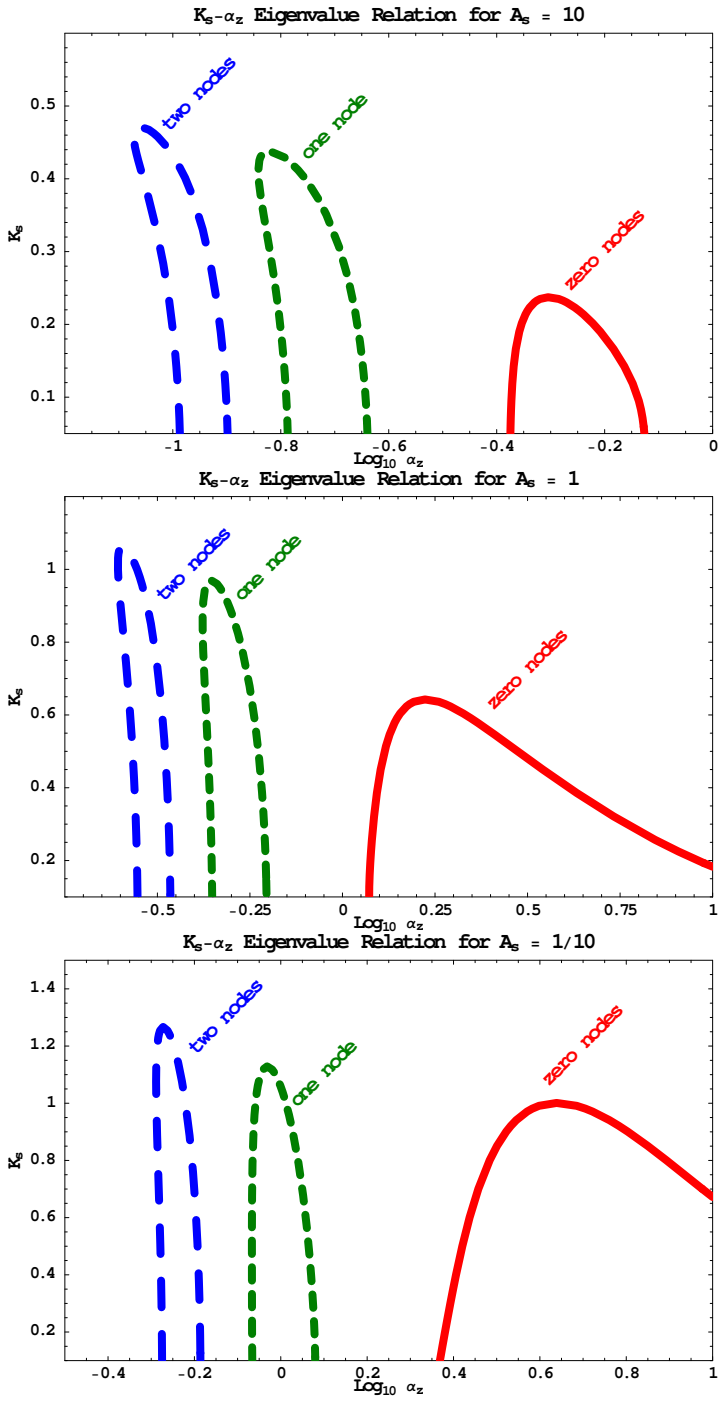

A more explicit map of the eigenvalue $K_s - \alpha_z$ relation for the linear smoothing operator *linear #1*, varying A_s while keeping $\lambda_0 = \Gamma_0 \delta_1 = 10^{-3}$ and $\delta_1 = 10^{-3}$ constant. As first shown in [5], as A_s increases (magnetic energy dominating over thermal energy), the modes have decreased K_s and they exist at lower α_z – hence in a more toroidal field. Equivalently, for all three nodal eigenvalues, as A_s, the K_s decreases – hence the parallel wavenumber $k_\parallel$ becomes smaller.

Furthermore, especially for large A_s it appears that there exist "double" solutions – two values of K_s for a given growth rate Γ_0 and equilibrium field, represented by α_z – a result that could not be easily observed in previous work on marginally stable 3D modes [5, 7].

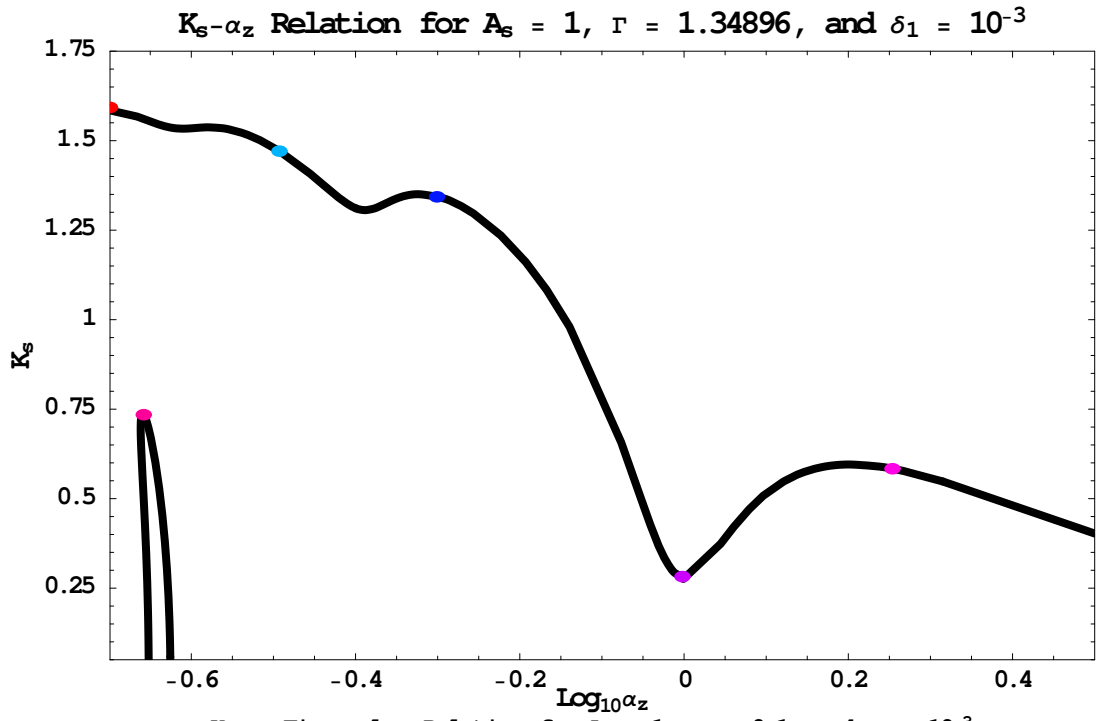

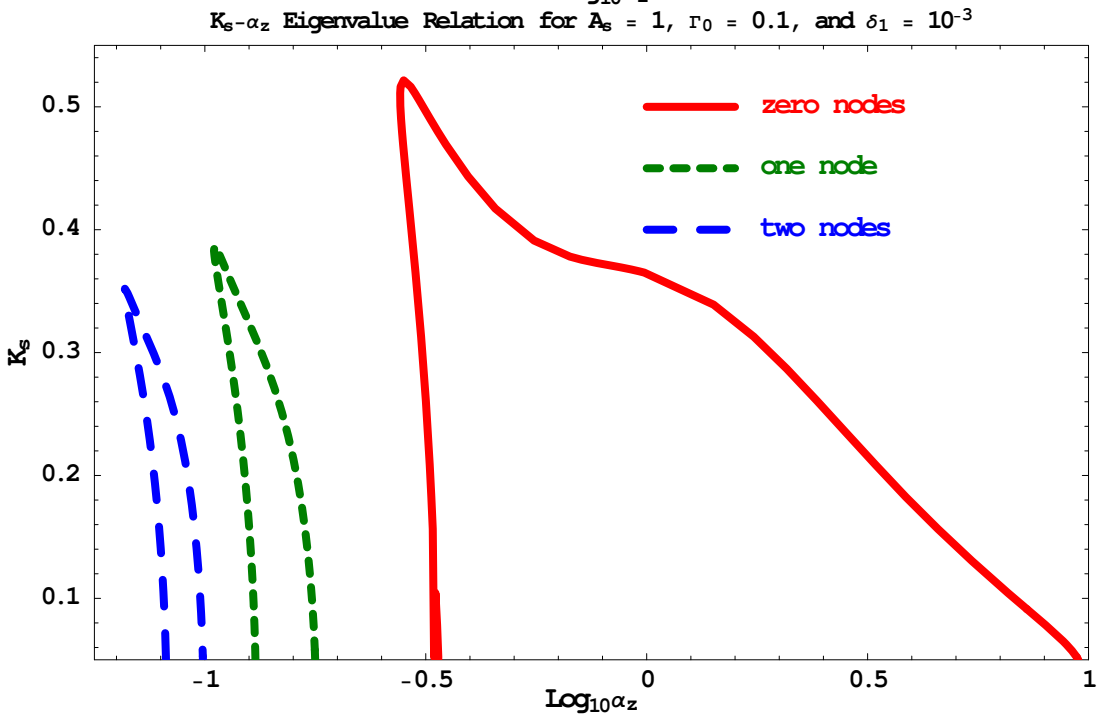

The $K_s - \alpha_z$ relation for the linear smoothing operator *linear #1*, for the case where $\lambda_0 = 10\delta_1 = 10^{-2}$ (on top, high growth rate) and for the case where $\lambda_0 = 0.1\delta_1 = 10^{-4}$ (on bottom, low growth rate), keeping $A_s = 1$. ***Note that the shapes of the high growth rate and low growth rate look substantially different from the $\Gamma_0 = 1$ case – in the case of high growth rate, there appear to be a class of solutions that are continuously connected from zero radial nodes, to one radial node, on up.***

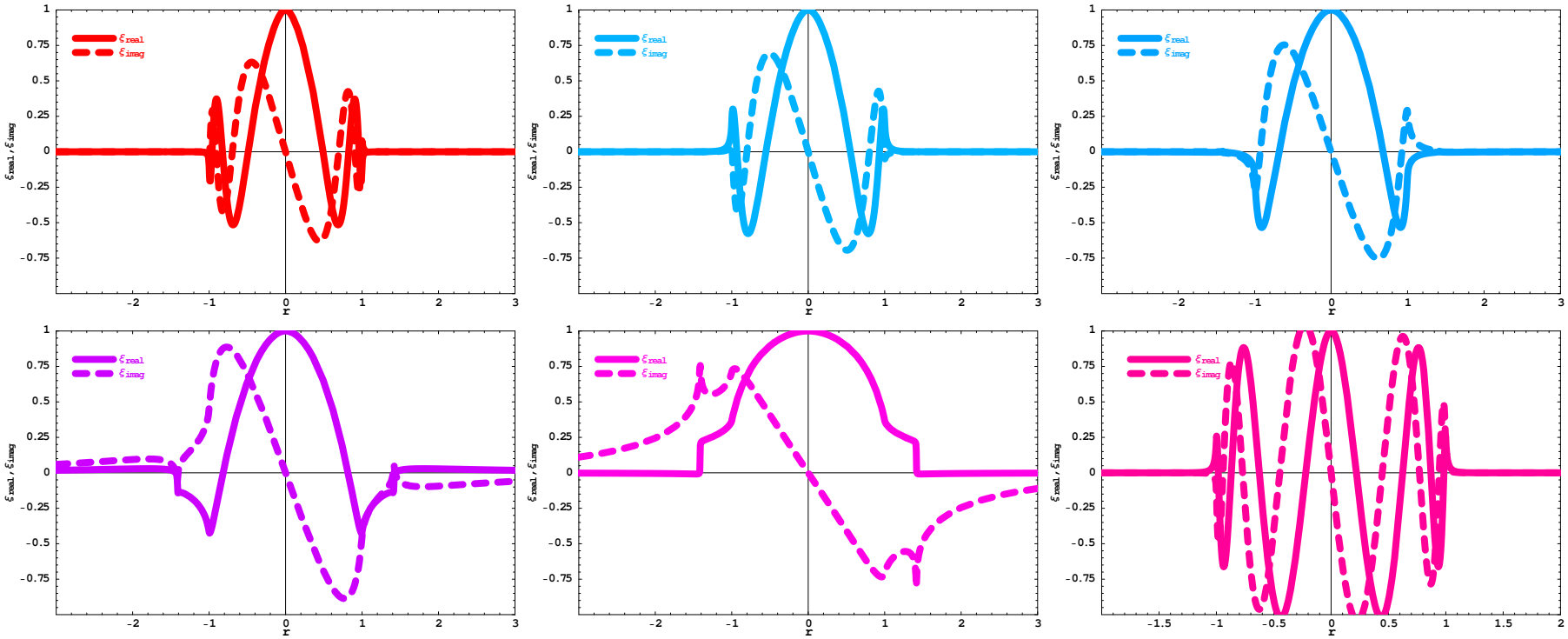

The various eigenmodes for the large growth rate case $\Gamma_0 = 10^{0.13}$ in a 3D modal equation described by nonlinear dissipation, *nonlin #2*. Each eigenmode, from the first to the fifth as one moves left and downwards, corresponds in color and position as one moves on the upper K_s branch of the large Γ_0 $K_s - \alpha_z$ eigenmode graph from smaller α_z (red) to larger α_z (magenta). Furthermore, the fourth plot in the sequence (corresponding to the point on the upper K_s branch at a local minimum) appears to be a "transitional" eigenmode – it has one radial node but is close to two radial nodes.

The final plot corresponds to the single point identified on the lower K_s branch of the same $K_s - \alpha_z$ eigenmode plot, and appears to have three radial nodes. The nature of the fundamental change in $K_s - \alpha_z$ relation for *nonlin #2* smoothing operator is unknown, but may occur for some threshold $\Gamma_0 > 1$.

Results and Conclusions

- A comparison of the eigenmodes of the 3D equation, as A_s is varied from small $A_s < 1$ to large $A_s > 1$ (corresponding to negligible to significant magnetic energies relative to thermal energies), and as growth rate Γ_0 is varied from small to large, reveal similar behaviors between the linear dissipative transition model *linear #1* and the nonlinear diffusive transition model *nonlin #1*; both *linear #1* and nonlinear model *nonlin #1* have a trend in allowable K_s and α_z, as A_s and growth rate are varied, as described for a class of linear transition models [7].

- The nonlinear dissipative model *nonlin #2* has a behavior of the eigenmodes K_s, as evidenced by the $K_s - \alpha_z$ eigenmode plot, that is unusual as growth rate is increased for some $\Gamma_0 > 1$, especially the agglomeration of several separate nodal solutions for smaller Γ_0 into a single higher K_s branch.

- As $\Gamma_0 \to 0$, the eigenvalue plots of the transition models do not converge. This is due to the fact that as $\Gamma_0 \to 0$, $\mathcal{I}(\Gamma_0)$, proportional to the jump in the derivative of $\tilde{\xi}_I$ across the first singularity $r = 1$, approaches 1/3 for *linear #1* transition model, but approaches 0 for both nonlinear models.

  - However, the nonlinear models also have different "shapes" in their respective $K_s - \alpha_z$ graphs, as well as different central values of α_z and maxima of K_s, for a given growth rate, although their corresponding values of $\mathcal{I}$ are separated by order ~ 1.

  - This implies that other features besides the characteristic parameter $\mathcal{I}$, such as the maxima and extent of Z_I, may also play a role; an example that was alluded to in [7, 12] is the fact that "double-humped" transition functions Z_I, such as in *linear #1*, may be different from "single-humped" Z_I as in *nonlin #1* and *nonlin #2*.

- Although nonlinear models of the transition may be justifiable due to the fact that pressure, density, etc.

go to infinity at the inner transition region in the MHD approximation [6, 10, 8]; however a linear model of the transition is more tractable mathematically, since modes are independent of each other.

- The study of a spectrum of modes is hampered by the fact that since the physical mechanism resulting in linear or nonlinear transitions is unknown, then mathematically **the behavior of the transition layer width δ_1 as a function of other parameters of the system (e. g., K_s, A_s, and total wavenumber) is not known. The growth rate as a function of the parameter K_s as described in [7] is valid only if δ_1 is kept as a constant.**

  – For nonlinear operators, the phenomenological fluid displacement L_N, at which nonlinear effects become important, is determined by whether finite pressure (thermal energy density) or finite momentum density of a given eigenmode are more important.

  – As an example, if linear transitions are determined solely by collisional diffusion effects (such as collisional thermal conductivity, kinetic ion viscosity, or electrical resistance), so that the physical radial extent of the transition region becomes $\Delta_1 = \left(D_T / \left[2k_z \Omega \alpha_z\right]\right)^{1/3} \ll \omega_{A_s}$, then one can show that from the given substitutions:

$$\delta_1 \equiv \text{ratio of scale of mode to scale of transition region} = K_s^{-1} \left(k/k_0\right)^{2/3} \alpha_z^{1/3} \left(1 + 4\alpha_z^2/9\right)^{1/6} \ll 1$$

$$k_0 H = \left(\frac{D_T}{c_S H}\right)^{-1/2}$$

  Thus, δ_1 is some nontrivial combination of the modal width δ_0 and the fixed modal properties (i.e., magnetic field, sound velocity, disk height).

- Since the exact form of the relationship between δ_1 and the other parameters of the problem are not well-known, δ_1 may also need to be varied – **an extra level of dimensionality**.

References

[1] E. Velikhov, Sov. Phys.–JETP **36**, 995 (1959).

[2] S. Chandrasekhar, Proc. Nat. Acad. Sci. USA **46** (1960).

[3] S. A. Balbus and J. Hawley, Astrophys. J. **400**, 610 (1992).

[4] N. I. Shakura and R. A. Sunyaev, Astron. & Astrophys. **24**, 337 (1973).

[5] R. Bhatt, B. Coppi, I. Dimov, and J. Gagnon, Bull. Amer. Phys. Soc. **45**, 38 (2000).

[6] B. Coppi and P. S. Coppi, Ann. Phys. (NY) **291**, 134 (2001).

[7] B. Coppi, R. Bhatt, and I. Dimov, Tech. Rep. PTP-01/01, M. I. T. (R. L. E.) (2001).

[8] B. Coppi and P. S. Coppi, Tech. Rep. PTP-01/04, M. I. T. (R. L. E.) (2001).

[9] B. Coppi and E. A. Keyes, Tech. Rep. PTP-02/02, M. I. T. (R. L. E.) (2002).

[10] B. Coppi and P. S. Coppi, Phys. Rev. Lett. **87**, 051101 (2001).

[11] R. Matsumoto and T. Tajima, Astrophys. J. **445**, 767 (1995).

[12] I. Dimov, B. Sc. Thesis, M. I. T., Cambridge, MA (2002).